Seventh International Conference on CFD in the Minerals and Process Industries
CSIRO, Melbourne, Australia
9-11 December 2009

WALL Y$^+$ APPROACH FOR DEALING WITH TURBULENT FLOW OVER A SURFACE MOUNTED CUBE: PART 1 – LOW REYNOLDS NUMBER

Mohd ARIFF, Salim M. SALIM* and Siew Cheong CHEAH

Department of Mechanical, Materials and Manufacturing Engineering,
University of Nottingham (Malaysia Campus), Semenyih, 43500, Selangor, MALAYSIA
*Corresponding Author, Email address: keyx8sms@nottingham.edu.my

ABSTRACT

An approach for dealing with turbulent flows over a surface-mounted cube using the wall y^+ as guidance in selecting the appropriate grid configuration and corresponding turbulence models are investigated using Fluent. The study is divided into two parts - Part I and Part II, dealing with low and high Reynolds numbers, respectively. In Part I presented here, a Reynolds number of 1,870 based on cube height and bulk velocity is investigated and the computation results are compared with data from Meinders et al. (1999) on 'the experimental study of local convective heat transfer from a wall-mounted cube in turbulent channel flow.' The standard *k-ε*, standard *k-ω*, Reynolds Stress Model (RSM), Spalart-Allmaras (SA) and renormalization group (RNG) *k-ε* turbulence models are used to solve the closure problem. Their behaviours together with the accompanying near-wall treatments are investigated for wall $y^+\approx1$ covering the viscous sublayer and $y^+\approx7$ in the buffer region. Notably, adopting a wall y^+ in the log-law region, where $y^+ >30$, would result in a poor mesh resolution due to the low Reynolds number of the main flow but is taken into consideration in the high Reynolds number flow case (Part 2 – Ariff et al., 2009). Overall, SA gave better agreement with experimental data and predicted the re-attachment length similar to DNS results as reported by Alexandar et al. (2006).

NOMENCLATURE

D	Domain Depth (m)
H	Height of Obstacle (m)
L	Length of the channel (m)
u	Instantaneous Velocity (ms^{-1})
u_B	Bulk Velocity (ms^{-1})
u_τ	Friction Velocity (ms^{-1})
x	Horizontal Distance along Streamwise direction (m)
X_F	Front Separation Length (H)
X_R	Reattachment Length (H)
y	Vertical Distance normal to wall direction (m)
z	Distance parallel to the spanwise direction (m)
Re_H	Reynolds Number ($=Hu_B/\upsilon_{air}$)
y^+	Dimensionless distance to the wall
k	Turbulent kinetic energy ($m^2 s^{-2}$)
ν_{air}	Kinematic viscosity of air ($m^2 s^{-1}$)
ω	Specific dissipation rate
ε	Dissipation rate

INTRODUCTION

The majority of time spent in a Computational Fluid Dynamics (CFD) project is usually devoted to successfully generating a mesh for the domain, as noted by Jinyuan et al. (2006), allowing a compromise between the desired accuracy and solution cost. This time-consuming procedure is considered a bottleneck in the analysis.

The preferred method for determining the most accurate mesh is to carry out test runs on different mesh sizes and configurations and match the converged numerical solution as closely as possible to experimental data, in what is termed the *grid independence test*.

Turbulent flows are significantly affected by the presence of walls, where the viscosity-affected regions have large gradients in the solution variables and accurate presentation of these regions determines successful prediction of wall bounded flows (Gerasimov, 2006).

Salim and Cheah (2009) succeeded in drawing up recommendations for best mesh practices based on the computed wall y^+ for cases where reliable experimental data may not be available for validation. Their study was carried out for a two-dimensional (2D) problem covering both undisturbed and disturbed turbulent flows over a solid-ridge bounded by a flat smooth wall at Re_H=17,000 based on the flow mean velocity and ridge height. The recommendations include the behaviour and suggested usage of the inbuilt Reynolds averaged Navier-Stokes (RANS) models and near-wall treatments using Fluent.

Due to the complexity of turbulence which is three-dimensional (3D) in nature, the present study covers the turbulent flow around a wall-mounted cube which has been extensively studied experimentally by Meinders et al. (1999) for a developing turbulent channel flow with low Reynolds numbers of $2{,}750<Re_H<4{,}970$. The case was chosen due to its simple geometry but complex flow structures and represents a general engineering configuration that is relevant to many engineering applications ranging from prediction of wind loading on structures to cooling of turbines and electronic components in circuit boards.

Similarly, a significant number of numerical studies using simple RANS models such as *k-ε* by Lakehal and Rodi (1997) and Gao and Chow (2005), unsteady RANS by Iaccarino et al. (2003), large eddy simulation (LES) by

Shah and Ferziger (1997) and the more complicated Direct Numerical Analysis (DNS) by Alexander et al. (2006) have been performed for such a flow configuration that has been widely used for bench-marking purposes to validate turbulent models and numerical methods. Recently, Ratnam and Vengadesan (2008) included heat transfer for the same flow case.

In all the numerical analyses, particularly those using RANS formulation, the accuracy of the results were dependent on the turbulence models used, near-wall treatments applied, discretization schemes employed, convergence criteria set, among other solver factors. This study addresses the selection of best mesh and the accompanying turbulence models and near-wall treatments using Fluent, which is particularly helpful as guidance for situations where experimental validation may not be available or for initial design considerations where alternative experimentation is expensive.

The wall y^+ [equation (1)] is a non-dimensional number similar to local Reynolds number, determining whether the influences in the wall-adjacent cells are laminar or turbulent, hence indicating the part of the turbulent boundary layer that they resolve.

$$y^+ = \frac{u_{\tau air} y}{\nu_{air}} \quad (1)$$

The subdivisions of the near-wall region in a turbulent boundary layer can be summarized as follows (Fluent, 2005):

(a) $y^+ < 5$: in the viscous sublayer region
(velocity profiles is assumed to be laminar and viscous stress dominates the wall shear)
(b) $5 < y^+ < 30$: buffer region
(both viscous and turbulent shear dominates)
(c) $30 < y^+ < 300$: Fully turbulent portion or log-law region (corresponds to the region where turbulent shear predominates)

MODEL DESCRIPTION

The computational domain as presented in Figure 1 is used for the present study to mimic the experimental setup of Meinders et al. (1999) for a turbulent channel flow and is similar to the geometry configurations implemented by Alexander at el. (2006) and Ratnam and Vengadesan (2008) in their respective studies. In these studies, the Reynolds number, based on channel height and bulk velocity, u_B, is predominantly 5,610.

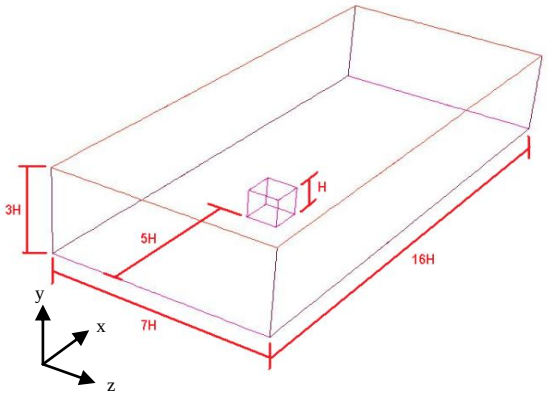

Figure 1: Schematic diagram of geometry.

Incompressible 3D steady flow RANS equations are used in this study which is available in reference texts (Pope, 2000 and Wilcox, 2006). The governing equations for the standard k-ε, standard k-ω, RSM, SA and (RNG) k-ε models can be found in Fluent 6.3 (2005).

The grid is constructed using the pre-processer GAMBIT to discretize the geometry domain before exporting it to Fluent, which then discretizes and solves the governing equations. Figure 2 represents Mesh 1 with the first cell height of 0.01H, grid size of 130 x 78 x 120 and a total of approximately 1.2 million cells. Mesh 2, with first cell height 0.1H, grid size of 56 x 22 x 50 and nearly fifty thousand cells is illustrated in Figure 3. The successive ratios for both meshes are 1.10, 1.02 and 1.10 in x-, y- and z-direction, respectively. The use of the two different mesh configurations allows us to study the behaviour of different turbulence models and near-wall treatments for two sets of y^+, resolving the viscous sublayer and the buffer region, respectively. In order to resolve the turbulent region of the boundary layer, i.e. y^+ above 30, the first cell height is required to be greater than 0.5H which is not practical as the other flow characteristics will not be appropriately accounted for due to the coarse grid.

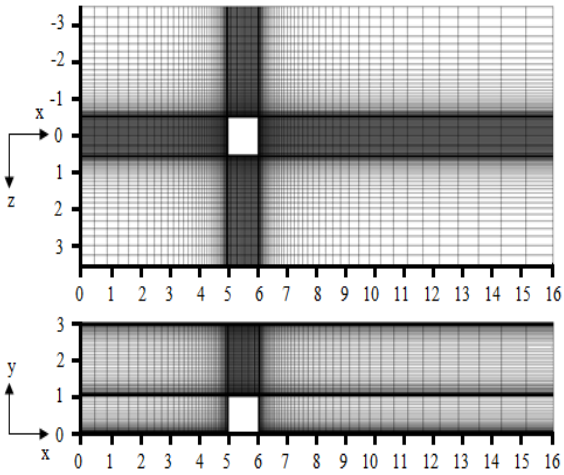

Figure 2: Computational grid (Mesh 1) used for present study.

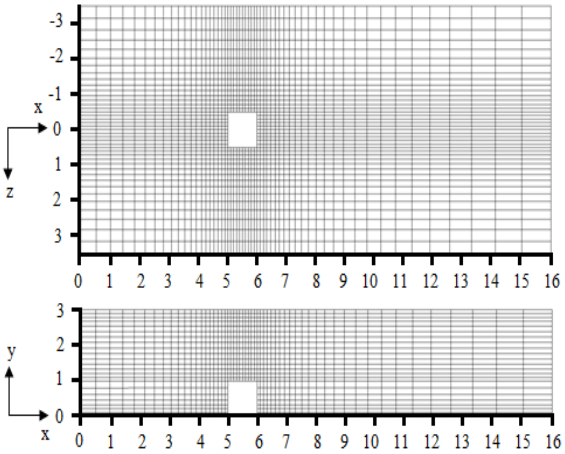

Figure 3: Computational grid (Mesh 2) used for present study.

A fully developed mean velocity profile is set at the channel inlet to replicate work by Alexander et al. (2006) and identical to the benchmark simulations of Kim et al. (1987). This was achieved by first running the simulation in an empty domain and implementing the fully developed velocity profile into the boundary condition of the presented case domain. A Reynolds number of 1,870 based on cube height and bulk velocity is realised, as compared to the lower limit of 2,750 for the developing channel flow investigated by Meinders et al. (1999).

A symmetry boundary condition is used for the side walls of the channel in order to reduce the computational cost, as the distance of the walls are sufficiently far from the cube to influence the flow. A pressure outlet is set for the exit faces while the remaining faces, i.e. the top and bottom walls including all faces of the cube are defined as smooth walls.

RESULTS

Mesh Configuration

The corresponding y^+ values obtained using standard k-ε with standard wall function (SWF) for Mesh 1 and Mesh 2 are ≈ 1 and 7, which resolves the viscous sublayer and buffer regions, respectively. These are shown graphically in Figure 4. The fluctuation in the curves is due to the presence of the obstacle in the flow path.

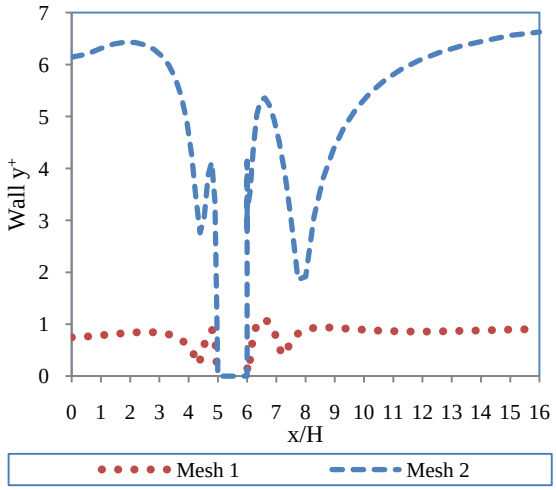

Figure 4: Wall y^+ for the considered Meshes.

Figure 5 and Figure 6 show the computed mean velocity profiles at two different locations (y/H = 0.1 and y/H = 0.9, respectively) validated against experimental data provided by Meinders et al. (1999) using the standard k-ε model. As can be seen from the figures, Mesh 1 computed the velocity profiles more accurately as compared to Mesh 2 due to the fact that Mesh 1 was much finer hence able to capture the large gradients in the region adjacent to the wall. This further indicates why a coarser mesh that would resolve the log-law region is not acceptable and not recommended for relatively low Reynolds number, such as Re_H = 1,870. However, the prediction of reverse flow at the front face of the cube is less successful for both meshes.

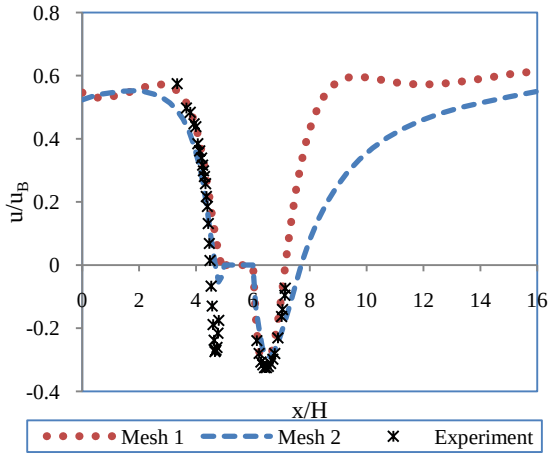

Figure 5: Comparison of mean streamwise velocity in the symmetry line near wall region y/H=0.1. Re_H = 1,870.

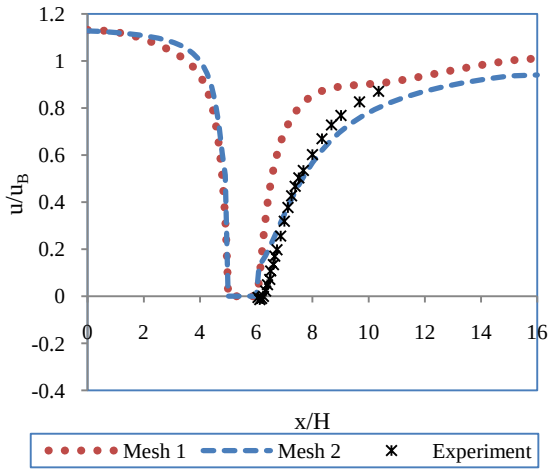

Figure 6: Comparison of mean streamwise velocity in the symmetry line far from wall y/H=0.9. Re_H = 1,870.

Turbulence Model and Near-Wall Treatment

Figure 7 shows the comparison of mean streamwise velocity profiles in the symmetry line at 5 different heights (y/H = 0.1, 0.3, 0.5, 0.7 and 0.9) to illustrate the performance of different turbulence models for the selected Mesh 2 with $y^+ \approx 1$. RSM only did particularly well in predicting the reverse flow at the front face at y/H = 0.1, whereas it overpredicts the reattachment region behind the cube. Overall, the SA models gives better agreement with experimental results, particularly at y/H=0.1 and 0.3. This is because SA is a two-zonal model, requiring no wall-functions to bridge the solution variables from the first cell to the adjacent wall and operates better if the viscous sublayer is resolved as with the case of the chosen Mesh. Beyond y/H=0.5, all the models underpredicted the velocity profiles except for RSM which overpredicts and is only slightly enhanced by either using the improved turbulence models implemented by user-defined functions and unsteady flow predictions (Ratnam and Vengadesan, 2008) or using the more computationally expensive DNS (Alexander et al., 2006). The results show that the use of inbuilt RANS models available in Fluent can achieve reasonable predictions, provided the required computational time and resources are taken into consideration.

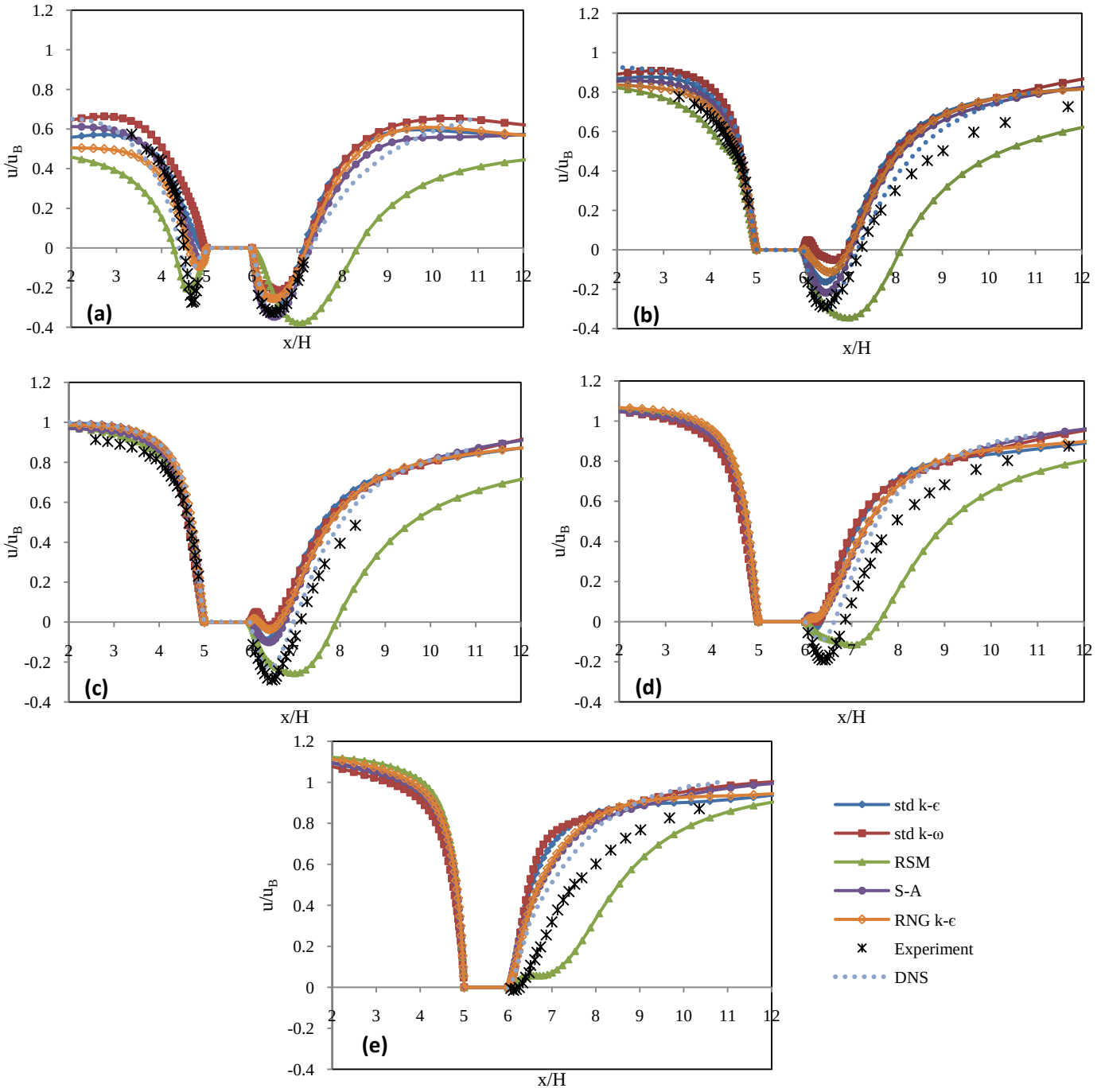

Figures 7: Comparison of the mean streamwise velocity profiles in the symmetry line; (a) y/H=0.1, (b) y/H=0.3, (c) y/H=0.5, (d) y/H=0.7 and (e) y/H=0.9, for Re_H = 1,870. Legends are same in all the plots.

Finally, Figure 8 shows the comparison of streamlines obtained by the different turbulence models employed in this study with DNS (Alexander et al., 2006) in the symmetry line x/H=0, and the experiment (Meinders et al., 1999) on the first grid point from the bottom wall. Streamlines are used to visualize the separation, recirculation and reattachments in the mean flow in front, on top, along the lateral sides and behind the cube. There is a horseshoe vortex in front of the cube, recirculation regions on top and behind the cube and side vortices; all accompanied by secondary vortices. Meinders at al. (1999) gives a more detailed description of the streamline patterns.

The streamlines suggests that the vortex structures predicted by all the models vary from one another in terms of location and size, especially in the flow separation, wake and recovery. The patterns look quite similar upwind and near the front face of the cube, but as discussed earlier the reverse flow in this area was underpredicted by all the models except for RSM. The same inadequacy is evident on top of the cube. SA computes sufficiently the recirculation zone downwind behind the cube, which is the most critical area, and predicts best the location of the arc vortex and the reattachment length similar to the DNS results, as summarized in Table 1.

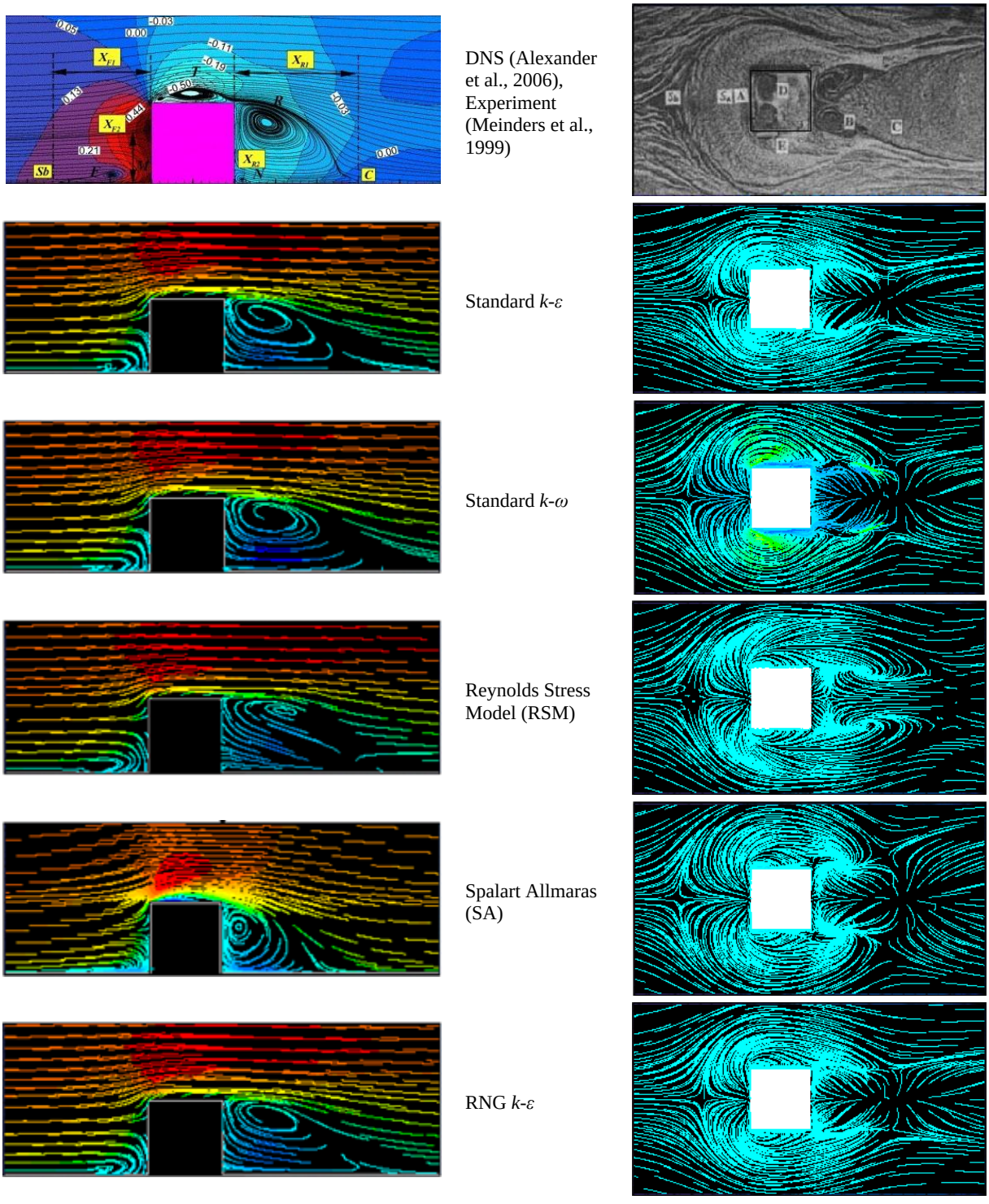

Figure 8: Comparison of streamlines in symmetry plane (left) z/H=0 and (right) first cell from bottom wall. Re_H = 1,870.

Turbulence Model	$X_F(H)$	$X_R(H)$
Experiment (Meinders et al., 1999)	1.24	1.44
DNS (Alexander et al., 2005)	1.2	1.5
Std k-ϵ (SWF)	0.64	1.29
Std *k-ω*	1.12	1.63
RSM	0.98	2.48
SA	1.20	1.56
RNG *k-ε*	0.81	1.49

Table 1: Summary of front separation (X_F) and reattachment lengths (X_R) for a wall mounted cube by different turbulence models.

It should be noted that other possible reasons for the discrepancies between the experimental and simulated results may be due to the different inflow conditions, namely, the fully developed channel flow used by the authors [similar to DNS study of Alexander et al. (2006) and experimental investigation of Kim et al. (1987)] in comparison to those of the developing flow in Meinders et al. (1999); apart from the choice of turbulence model, discretization scheme and mesh configuration.

CONCLUSION

The present study provides guidance on selecting the appropriate mesh configuration and turbulence model based on the computed wall y^+ for cases where experimental data are not available for validation and is suitable for initial design considerations and product development of projects dealing with comparatively low Reynolds numbers for wall bounded turbulent flows.

Different mesh configuration and RANS turbulence models were tested. Due to the low Reynolds number of the flow, only the wall y^+ resolving the viscous sublayer and buffer regions were investigated and it is not recommended to have a large first cell height covering the log-law region. A wall y^+ resolving the viscous sublayer in this case is deemed a better choice, as it is advisable to avoid resolving into the buffer region, since neither wall-functions nor near-wall modelling accounts for it accurately.

In Fluent, the Spalart-Allmaras turbulence model was sufficiently accurate when solving at a relatively low Reynolds number, steady flow problems using the RANS equations, considering a compromise between computational resources and sensitivity of prediction. This is due to the fact that it is a two-zonal model that requires no wall-functions to bridge it to the solution variables at the wall, unlike *k-ε* and RSM. The wall-functions do not perform particularly well in the viscous sublayer since they are formulated predominantly for the log-law region.

REFERENCES

ALEXANDER, Y., LUI, H., and NIKITIN, N., (2006), "Turbulent flow around a wall mounted cube: A direct numerical simulation", Int. J. Heat and Fluid Flow 27, 994-1009.

ARIFF, M., SALIM, S.M., and CHEAH, S.C., (2009), "Wall Y^+ Approach for Dealing with Turbulent Flow over a Surface Mounted Cube: Part 2 – High Reynolds number", Proc. Int. Conf. on CFD in the Minerals and Process Industries, CSIRO, Melbourne, Australia, December.

FLUENT (2005), *Documentation: User guide*, ANSYS Inc.

GAO, Y., and CHOW, W.K. (2005), "Numerical studies on air flow around a cube", J. Wind Eng. and Ind. Aerodynamic 93, 115-135.

GERASIMOV, A., (2006), "Modelling Turbulence Flows with Fluent", Europe ANSYS Inc.

IACCARINO, G., OOI, A., and BEHNIA, M., (2003), "Reynolds averaged simulation of unsteady separated flow", Int. J. Heat and Fluid Flow 24, 147-156.

JINYUAN, T., GUAN, H.Y. and CHAOQUN, L., (2006), *Computational Fluid Dynamics: A Practical Approach*, USA: Butterworth-Heinemann.

KIM, J., MOIN, P., MOSER, R., (1987), "Turbulence statistics in fully developed channel flow at low Reynolds number", J. Fluid Mech. 177, 133-166.

LAKEHAL, D., and RODI, W., (1997), "Calculation of the flow past a surface of a mounted cube with 2-layer turbulence model", J. Wind Eng. and Ind. Aerodynamics 67-68, 65-78.

MEINDERS, E.R, HANJALIC, K., and MARTINUZZI, R., (1999), "Experimental study of the local convective heat transfer from a wall mounted cube in turbulent channel flow", Trans ASME J. Heat Transfer 121, 564-573.

POPE, S.B., (2000), *Turbulent Flows*, Second Edition, Cambridge University Press.

RATNAM, G.S., and VENGADESAN, S., (2008), "Performance of two equation turbulence models for prediction of flow and heat transfer over a wall mounted cube", Int. J. Heat and Mass Transfer 51, 2834-2846.

SALIM, S.M., and CHEAH, S.C., (2009), "Wall Y^+ Strategy for Dealing with Wall-bounded Turbulent Flows", Proc. Int. MultiConference of Eng. and Comp. Scientists, IMECS 2009, Vol II, Hong Kong, March.

SHAH, K.B. and FERZIGER, J.H. (1997), "A fluid mechanicians view of wind engineering: Large eddy simulation of flow past a cubic obstacle", J. Wind Eng. and Ind. Aerodynamics 67-68, 211-224.

WILCOX, D.C., (2006) *Turbulence Modelling for CFD*, Third Edition, DCW Industries.

